Chinese Journal of
POLYMER SCIENCE

RESEARCH ARTICLE

https://doi.org/10.1007/s10118-025-3375-x
Chinese J. Polym. Sci. **2025**, *43*, 2160–2170

Effects of Solvent Qualities on the Conformation of a Homopolymer Chain in Binary Mixed Solvents

Liang-Sen Bai and Peng-Fei Zhang*

State Key Laboratory of Advanced Fiber Materials, Center for Advanced Low-Dimension Materials, College of Materials Science and Engineering, Donghua University, Shanghai 201620, China

Abstract The chain conformation of polymers in binary solvent mixtures is a key issue in the study of functional soft matter and lies at the heart of various applications such as smart soft materials. Based on a minimal lattice model, we employ Monte Carlo (MC) simulation to systematically investigate the effects of solvent qualities on the conformation of a single homopolymer chain in binary mixed solvents. We also perform calculations using a Flory-type mean-field theory. We focus on how the introduction of a second solvent B affects the dependence of chain conformation on the quality of solvent A. We mainly examine the effects of the composition of solvent B, denoted by x, and the interactions between the two solvents. First, when x is low, the mean-square chain radius of gyration exhibits qualitatively similar behaviors to those in an individual solvent A, with a slight chain contraction when solvent A is very good. Second, in equal-molar mixtures with x=0.5, a homopolymer chain collapses when solvent A is either poor or very good, while expands at intermediate qualities. Lastly, at large x, a chain undergoes a coil-to-globule transition with the increasing quality of solvent A when solvent B is good, but mainly adopts the collapsed conformation when solvent B is poor. Our findings not only improve our understanding on the chain conformation in binary solvent mixtures, but also provide valuable guidance on the rational design of stimuli-responsive polymeric materials.

Keywords Binary mixed solvents; Monte Carlo simulation; Conformation; Solvent quality; Mean-field theory

Citation: Bai, L. S.; Zhang, P. F. Effects of solvent qualities on the conformation of a homopolymer chain in binary mixed solvents. *Chinese J. Polym. Sci.* **2025**, *43*, 2160–2170.

INTRODUCTION

The coil-to-globule transition of polymers in solution is one of the most important phenomena in polymer science and has been widely used in various applications such as stimuli-responsive polymers,[1–4] polymer films and membranes,[5–7] and bioadhesives.[8–10] Solvent quality is one of the key factors affecting the polymer chain conformation. In a single solvent, the coil-to-globule transition caused by the change in solvent quality has been well understood.[11–16] However, in binary solvent mixtures, the combined effect of the two solvents leads to many complex and interesting phenomena,[17–25] and one of the most intriguing phenomena is the co-nonsolvency effect[19–20,26–33] that refers to the collapse of a single polymer chain in a mixture of two miscible good solvents. The co-nonsolvency effect has been observed in many polymer systems, such as poly(N-isopropylacrylamide) (PNIPAM) in water/methanol mixtures[19,20,34–39] and elastin-like polypeptides in water/ethanol mixtures,[40] and this effect is extensively used in many fields such as block copolymer self-assembly,[41,42] nanoparticle preparation,[43] and smart brush design.[44–50] Understanding the synergistic effects of the solvent quality in binary solvent mixtures on the chain conformation is crucial for such applications based on mixed solvents. Currently, there are two main viewpoints on the mechanisms of the co-nonsolvency effect.[20,26–27,29–31,33,36,44,45,51–74] The first one regards that the attraction between the two solvents or the solvent-cosolvent complex formation is the key factor leading to chain collapse.[20,30,31,52,66,70] For example, Zhang and Wu speculated that the methanol and water molecules form pentagon clusters that are poor to PNIPAM, and thus, drives the chain collapses at intermediate compositions of methanol.[20] The second viewpoint, on the other hand, attributes the co-nonsolvency effect to the preferential adsorption of one solvent onto the polymer backbone induced by the significant difference in the solvent quality between the two solvents;[26,55,63,69–70,72–75] one typical example is the concept of cooperative hydration proposed by Tanaka and his collaborators.[55,75]

Various molecular simulations, including both molecular dynamics (MD) and Monte Carlo (MC) simulation methods, have been used to examine the conformation transition of a homopolymer chain in mixtures of two solvents. For example, by treating both types of solvents explicitly, Kremer and coworkers employed both all-atomic and coarse-grained MD simulations to examine the conformation transition of a single homopolymer chain along the cosolvent composition.[26] They found that the chain collapses over an intermediate

* Corresponding author, E-mail: pfzhangphy@dhu.edu.cn
Received April 10, 2025; Accepted May 4, 2025; Published online July 29, 2025

range of the cosolvent composition when the solvent qualities of the two good solvents differ significantly, and thus, proposed that the co-nonsolvency is a generic phenomenon driven by preferential adsorption. Later on, Sommer and coworkers also performed MD simulations to investigate the expansion–collapse–re-expansion transition of homopolymer brushes in mixtures of an implicit good solvent and an explicit good cosolvent.[44] Moreover, Zhang *et al.* employed the MD simulations to demonstrate that the co-nonsolvency effect can be utilized to fabricate single-chain nanoparticles with high sphericity and compactness.[43]

On the other hand, based on the simple cubic lattice model, Magda *et al.* carried out canonical MC simulations to study the conformation of a single homopolymer chain in binary mixed solvents.[76] They examined both mixtures of two good solvents and mixtures of a good solvent and a poor solvent. One notable finding is that, under the preferential adsorption conditions, a polymer chain may undergo a contraction transition when the quality of one solvent is sufficiently good. More recently, using the same lattice model, Zhang *et al.* also employed MC simulations to study the conformation of a single homopolymer chain in mixtures of two solvents A and B.[72] In particular, they developed an efficient and accurate MC technique to study the variation of the chain size along the quality of one solvent B while keeping all other interactions unchanged. One interesting observation is the non-monotonic variation of the chain size with increasing the quality of solvent B when solvent A is good. Specifically, at moderately small fractions of solvent B, a chain collapses if solvent B is poor but swell gradually with increasing the quality of solvent B. One surprising finding is that the chain may undergo a continuous collapse transition when the solvent B becomes sufficiently good.

It was assumed that the interaction between the two solvents A and B is zero in the work by Zhang and coworkers.[72] However, in real systems the interaction between solvents A and B, characterized by ε_{AB}, is hardly zero. Finite ε_{AB} definitely has an important effect on the conformation of homopolymer chains in mixtures of two solvents. Indeed, the systematic studies by Zhang, using the ternary Flory-Huggins theory, have demonstrated that the finite interaction between the two solvents plays an important role in regulating the bulk phase behaviours of homopolymer in mixtures of binary solvents.[73,74] Examining the effect of ε_{AB} will not only improve our understanding on the chain conformations of polymers in mixtures of binary solvents, but also offer valuable guidance on the rational design of smart materials based on mixed solvents. However, a comprehensive understanding of the influence of the interaction between the two solvents, ε_{AB}, on the chain conformation of polymers in mixed solvents, is still lacking.

To this end, this work aims to address how the introduction of a solvent B affects the dependence of the chain size on the quality of solvent A. We emphasize on the effects of the composition and qualities of solvent B, as well as the interaction between the two solvents. Specifically, based on a simple cubic lattice model with minimal parameters, we employ the MC method to explore the conformational changes along the quality of one solvent with all other parameters fixed. To further understand our MC simulation results, we also apply a Flory-type mean-field theory to study the chain conformations in mixtures of binary solvents. To the best of our knowledge, this work represents the first comprehensive study on the conformation transition of a single homopolymer chain in mixed solvents in the presence of finite ε_{AB}. In particular, we find that, in the equal-molar mixtures, a homopolymer chain collapses when solvent A is either poor or very good, while adopts an expanded coil conformation at intermediate qualities. When the solvent A is good, the range of the expanded coil conformation depends on ε_{AB} in a non-monotonic way.

Our paper is organized as follows. In **MODEL AND METHODS**, we introduce the lattice model for homopolymers in binary solvents and then recapitulate the details of the MC simulation technique and the Flory-type mean-field theory developed in Ref. [72]. In **RESULTS AND DISCUSSION**, we present the key results from MC simulations and theoretical calculations, focusing on the impact of the solvent qualities in the presence of finite interactions between the two solvents. Finally, in **CONCLUSIONS**, we summarize the main findings and also provide a brief outlook.

MODEL AND METHODS

In this work, we adopt the same model and methodology as developed in the work by Zhang and coworkers,[72] but focus on the effect of the quality of one solvent in the presence of a second solvent. In Ref. [72], it was found that a homopolymer chain in mixtures of binary good solvents undergoes a coil-globule-coil transition with increasing the composition of the better solvent. This observation is qualitatively consistent with the experimental observations by Zhang and Wu[20] and by Wang *et al.*[29] Although it is challenging to make quantitative comparison with these experiments due to the complexity of the experimental systems, the qualitative agreement suggests that our minimal model indeed captures all essential physics in the conformation of a homopolymer chain in mixtures of two solvents. Moreover, the simplicity of our model system allows us to systematically investigate the chain conformation and phase behaviors of homopolymers in binary mixtures in the huge parameter space. Hereafter we will first present the main ingredients of the lattice model and then recapitulate the primary procedures of both the MC simulation and the Flory-type mean-field theory.

Model

We model a homopolymer chain having N segments by a self-avoiding random walk on a simple cubic lattice of volume $V = L^3$ with L being the number of lattice layers in the x-, y-, and z-directions. We apply periodic boundary conditions in all three directions to mimic the bulk solutions. The lattice sites unoccupied by polymer segments are occupied by either solvent A or solvent B molecules. Assuming that each polymer segment and solvent molecule occupies one lattice site and each lattice site can be occupied at most by one segment or solvent molecule, we have $V = n_A + n_B + N$, where n_A and n_B are the total number of solvents A and B molecules, respectively. In Fig. 1, we present the schematics of our model system, where the red beads are polymer segment, the green and blue spheres denote the molecules of solvent A and B respectively. Moreover, the inter-

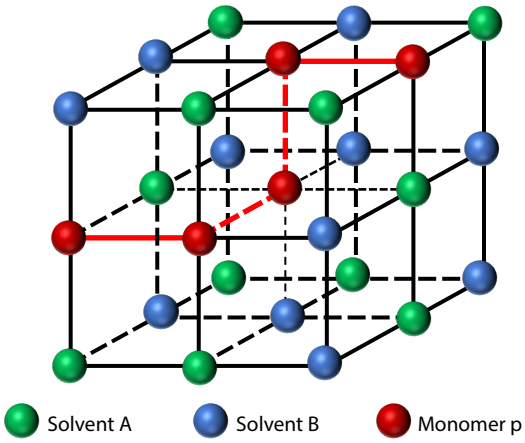

Fig. 1 Schematic illustration of a homopolymer chain immersed in a mixture of binary solvents A and B on the lattice model.

actions between different species are modelled by the nearest neighbour interactions on the lattice. Assuming the interaction for one nearest neighbour contact pair between species i and j by ε_{ij}, we have the non-bonded Hamiltonian as

$$H = \varepsilon_{pA}\hat{n}_{pA} + \varepsilon_{pB}\hat{n}_{pB} + \varepsilon_{AB}\hat{n}_{AB} \tag{1}$$

where $\hat{n}_{ij}$ denotes the total number of nearest-neighbor contact pairs between species i and j for one configuration. All interaction parameters are implicitly set in units of k_BT, where k_B is Boltzmann constant and T is the absolute temperature.

Under a given parameter set V, N, n_B, ε_{pA}, ε_{pB}, and ε_{AB}, the canonical partition function reads

$$\mathcal{Z}\left(n_B, \varepsilon_{pA}, \varepsilon_{pB}, \varepsilon_{AB}\right) = \frac{1}{n_A!n_B!}\int D\boldsymbol{R}\mathrm{d}\boldsymbol{r}_A\mathrm{d}\boldsymbol{r}_B\exp\left(-\varepsilon_{pA}\hat{n}_{pA} - \varepsilon_{pB}\hat{n}_{pB} - \varepsilon_{AB}\hat{n}_{AB}\right) \tag{2}$$

where $\boldsymbol{R} \equiv \{\boldsymbol{r}_1, \boldsymbol{r}_2, \ldots, \boldsymbol{r}_N\}$ represents the chain conformation with $\boldsymbol{r}_i$ denoting the spatial position of the i^{th} monomer. The configuration of solvent α is represented by $\boldsymbol{r}_\alpha = \{\boldsymbol{r}_{1,\alpha}, \boldsymbol{r}_{2,\alpha}, \ldots, \boldsymbol{r}_{n_\alpha,\alpha}\}$ where $\boldsymbol{r}_{i,\alpha}$ is the spatial position of the i^{th} solvent molecule of type α. The terms $n_A!$ and $n_B!$ account for the indistinguishability of solvents A and B, respectively. For given N and V, the chain conformation and thermodynamic properties of our system are determined by the following 4 parameters: ε_{pA}, ε_{pB}, ε_{AB}, and the composition of solvent B defined by $x = n_B/(n_A + n_B)$.

Monte Carlo (MC) Simulations

Given that the total number of configurations for large N is astronomically large, it is impractical to perform the summation in Eq. (2) exactly. We thus employ the MC simulation technique to study the conformation of a homopolymer in binary solvent mixtures. Specifically, we adopt the method developed by Zhang and coworkers[72] to rapidly calculate the restricted partition function in the space of monomer–solvent A contact number (denoted by n_{pA}) at fixed x, ε_{pB}, and ε_{AB}, and then examine the effect of the quality of solvent A, as denoted by ε_{pA}. To efficiently and accurately identify the possible conformational transitions along ε_{pA}, we rewrite the partition function as

$$\mathcal{Z}\left(\varepsilon_{pA}; x, \varepsilon_{pB}, \varepsilon_{AB}\right) = \sum\nolimits_{n_{pA}} \mathcal{X}\left(n_{pA}; x, \varepsilon_{pB}, \varepsilon_{AB}\right)\exp\left(-\varepsilon_{pA}n_{pA}\right) \tag{3}$$

where $\mathcal{X}$ is the restricted partition function defined as

$$\mathcal{X}\left(n_{pA}; x, \varepsilon_{pB}, \varepsilon_{AB}\right) \equiv \frac{1}{n_A!n_B!}\int D\boldsymbol{R}\,\mathrm{d}\boldsymbol{r}_A\,\mathrm{d}\boldsymbol{r}_B\exp\left(-\varepsilon_{pB}\hat{n}_{pB} - \varepsilon_{AB}\hat{n}_{AB}\right)\delta_{n_{pA},\hat{n}_{pA}} \tag{4}$$

The summation in Eq. (3) spans all possible n_{pA} values, and $\delta_{i,j}$ in Eq. (4) is the Kronecker delta function ($\delta_{i,j} = 1$ if $i = j$, and 0 otherwise). For brevity, we omit the variables x, ε_{pB}, and ε_{AB} in subsequent derivations. We use the generalized Wang–Landau algorithm[77,78] to compute $\mathcal{X}(n_{pA})$; we refer to Ref. [72] for the details of the algorithm. Once we obtain $\mathcal{X}(n_{pA})$, the ensemble-average of a physical quantities Q as a continuous function of ε_{pA} is calculated *via*

$$\langle Q\rangle = \frac{\sum_{n_{pA}}\overline{Q}\left(n_{pA}\right)\mathcal{X}\left(n_{pA}\right)\exp\left(-\varepsilon_{pA}n_{pA}\right)}{\mathcal{Z}\left(\varepsilon_{pA}\right)} \tag{5}$$

where $\overline{Q}(n_{pA})$ is the average of Q in the restricted ensemble and is given by

$$\overline{Q}\left(n_{pA}\right) \equiv \frac{1}{\mathcal{X}\left(n_{pA}\right)n_A!n_B!}\times \int D\boldsymbol{R}\,\mathrm{d}\boldsymbol{r}_A\,\mathrm{d}\boldsymbol{r}_B\,\hat{Q}\exp\left(-\varepsilon_{pB}\hat{n}_{pB} - \varepsilon_{AB}\hat{n}_{AB}\right)\delta_{n_{pA},\hat{n}_{pA}} \tag{6}$$

Here, $\hat{Q}$ denotes the instantaneous value of Q in a given configuration $\{\boldsymbol{R}, \boldsymbol{r}_A, \boldsymbol{r}_B\}$. Specifically, we use this method to compute the chain mean-square radius of gyration denoted by $\langle R_g^2\rangle(\varepsilon_{pA})$.

Generalized Flory-type Mean-field Theory

To gain deeper insights into our MC simulation results, we also employ the Flory-type mean-field theory to study the conformation of a homopolymer in binary solvent mixtures. This approach, initially proposed by Shultz and Flory[17] and then applied by other researchers,[44,46,59,72,79,80] is briefly reviewed here with a detailed reference to prior work.[72]

In this theory, the system is divided into two volumes with a region pervaded by the chain (with volume $V_i = (4/3)\pi R^3$ where R is the effective radius of this volume) and a solvent reservoir without polymer segments. The Helmholtz free energy density of the solvent reservoir given by the classical regular solution theory is

$$f_r l^3 = \phi_{Br}\ln\phi_{Br} + (1-\phi_{Br})\ln(1-\phi_{Br}) + \chi_{AB}\phi_{Br}(1-\phi_{Br}) \tag{7}$$

where ϕ_{Br} is the volume fraction of solvent B in the reservoir and l is the length of lattice spacing. In the mean-field approximation, χ_{AB} correlates with the parameter ε_{AB} in MC simulation *via* $\chi_{AB} = z_L\varepsilon_{AB}$ (with $z_L = 6$ being the lattice coordination number of the simple cubic lattice). Expressions for the exchange chemical potential of solvent B, μ_{Br}, and the osmotic pressure Π_r are provided in Eqs. (18) and (19) of Ref. [72].

On the other hand, the Helmholtz free energy F_i in the volume pervaded by the chain consists of the deformation free energy due to the conformation entropy and the Flory-Huggins mixing free energy,

$$F_i = \frac{9}{4}\left(\frac{6R_g^2}{Nb^2} + \frac{Nb^2}{6R_g^2}\right) + V_i\left[\begin{array}{c}\phi_B\ln\phi_B + \left(1-\phi_p-\phi_B\right)\ln\left(1-\phi_p-\phi_B\right) \\ + \chi_{pB}\phi_p\phi_B + \chi_{pA}\phi_p\left(1-\phi_p-\phi_B\right) \\ + \chi_{AB}\phi_B\left(1-\phi_p-\phi_B\right)\end{array}\right] \tag{8}$$

where the two terms in the parenthesis account for the deformation free energy due to chain expansion and contraction re-

spectively.[15,72] Specifically, the deformation free energy depends on the chain radius of gyration ($R_g = (3/5)^{1/2}R$). ϕ_p and ϕ_B are the volume fractions of polymer segment and solvent B in the volume pervaded by the chain, respectively. The mixing free energy density accounts for the mixing entropy of the two solvents and the interactions among the three species. Because we assume the centre of mass of the chain is fixed, there is no translational contribution from the chain. The Flory-Huggins parameter $\chi_{p\alpha}$ between the polymer and solvent α is linked to $\varepsilon_{p\alpha}$ in MC simulation by $\chi_{p\alpha} = (z_L - 2)\varepsilon_{p\alpha} = 4\varepsilon_{p\alpha}$. Expressions for the exchange chemical potential of solvent B, μ_B, and the osmotic pressure, Π, in the pervaded volume of the polymer chain are detailed in Eqs. (15) and (16) of Ref. [72].

By enforcing the equality of the chemical potential ($\mu_B = \mu_{Br}$) and osmotic pressure ($\Pi=\Pi_r$) for thermal equilibrium, we can numerically calculate the optimal R_g and internal composition of solvent B, ϕ_B. The thermodynamic potential of the system is then given by $G = F_i - \mu_{Br}\phi_B V_i + \Pi_r V_i$. When multiple solutions are encountered, we choose the physically relevant one with the lowest G.

RESULTS AND DISCUSSION

In this work, we choose N=100 and then use L=40 such that the finite-size effect is negligible. The chain conformation and thermodynamics of our system are thus determined by four parameters: ε_{pA}, ε_{pB}, ε_{AB}, and x. When x=0, our system reduces to a homopolymer chain in a single solvent A. The chain conformation of this system was examined by many groups and it is generally accepted that a chain undergoes a coil-to-globule transition with decreasing the quality of solvent A.[16,72,81–83] Specifically, for the simple cubic lattice model used here, the MC simulations by Zhang *et al.* identifies a coil-to-globule transition at $\varepsilon_{pA}\approx$0.142 and the chain mean-square radius of gyration therein is $\langle R_g^2\rangle\approx 0.278N$.[72] For N=100, we have $\langle R_g^2\rangle_0\approx$27.8 in the θ solvent. We thus regard a solvent A to be good when ε_{pA}<0.142 and poor otherwise. Likewise, a chain is regarded to be in the coil state when $\langle R_g^2\rangle$ is smaller than 27.8 and in the globule state otherwise. On the other hand, in the Flory-type mean-field theory, the solvent A is regarded to be good when χ_{pA}<0.5 and poor when χ_{pA}>0.5. Since the chain size is $\langle R_g^2\rangle_0$=20.06 when χ_{pA}=0.5 in single solvent A, we attribute the chain to be in the coil state when $\langle R_g^2\rangle$ is larger than 20.06 and in the globule state otherwise.[72] To quantitatively reveal the chain conformation in the mixed state in a transparent way, hereafter we define the reduced mean-square chain radius of gyration as $\langle R_g^2\rangle_r = \langle R_g^2\rangle/\langle R_g^2\rangle_0$ in both MC simulation and Flory-type mean-field theory. Then, a chain is classified to be in the coil state when $\langle R_g^2\rangle_r$ is larger than 1 and in the globule state otherwise.

Hereafter we focus on how the introduction of a second solvent B into a dilute homopolymer solution in solvent A affects the dependence of the reduced mean-square chain radius of gyration on the quality of solvent A, ε_{pA}. The introduction of solvent B brings into three more parameters: ε_{pB}, denoting the interaction between solvent B and polymer segment, ε_{AB} as the interaction between solvents A and B, and x representing the composition of solvent B. We note that the previous study by Zhang and coworkers have explored the polymer chain conformational changes with ε_{pA}, for the special case with ε_{AB}=0.[72] In this paper we extend that work by considering different interactions between the two solvents A and B. In particular, we choose three values of ε_{AB}, −0.6, −0.3, and 0.3, to represent the strong attraction, weak attraction, and repulsion between solvents A and B, respectively. We also include ε_{AB}=0 for comparison. As for the quality of solvent B, we choose ε_{pB}=−0.5 and ε_{pB}=0.2 to represent the good and poor solvent conditions for solvent B, respectively. Moreover, we choose the following three values of x to study the effects of different solvent composition: x=0.2, 0.5, and 0.95. For all cases, we also compare the MC simulation results with the predictions from the Flory-type mean-field theory with $\chi_{pA} = (z_L-2)\varepsilon_{pA} = 4\varepsilon_{pA}$, $\chi_{pB} = 4\varepsilon_{pB}$, and $\chi_{AB} = z_L\varepsilon_{AB} = 6\varepsilon_{AB}$. We note that the qualitative features of the chain conformation do not depend on the specific choices of these parameters.

Effect of the Quality of Solvent A at Small *x*

We first consider the situations when the composition of solvent B is small. By taking x=0.2 as an example, in Figs. 2(a) and 2(c) we present the reduced chain mean-square radius of gyration $\langle R_g^2\rangle_r$ as a function of ε_{pA} at ε_{pB}=−0.5 and 0.2 respectively from the MC simulations. These two ε_{pB} values corresponds to the good solvent and poor solvent conditions for the solvent B respectively. We also include $\langle R_g^2\rangle_r$ for the single-solvent case (*i.e.*, x=0) as the olive curve for comparison. As mentioned earlier, this single-solvent system has already been carefully examined in Ref. [72], and it is found that a homopolymer chain in the single solvent A adopts the expanded coil state when ε_{pA}<0.142 and the collapsed globule state when ε_{pA}>0.142. Both Figs. 2(a) and 2(c) show that the overall variation features of $\langle R_g^2\rangle$ along with ε_{pA} in mixed solvents remain roughly unchanged for both values of ε_{pB} with various ε_{AB}, with one exception that the chain may become slightly contracted with decreasing ε_{pA} in mixed solvents. This is understandable by noticing that the amount of solvent B is rather small here. Quantitatively, we observe several differences. First, when the solvent B is good, the size of the globule at large ε_{pA} in mixed solvent is slightly larger than that in pure solvent B while the size of the coil state at small (or negative) ε_{pA} in mixed solvents is somewhat smaller than that in pure solvent B; the magnitude of these variations is more pronounced when ε_{AB} is larger. Second, when the solvent B is poor, the chain size of the globule state in the mixed solvents is very close to that in pure solvent A, while the chain size of the coil state in the mixed solvents is smaller than that of pure solvent A. Third, with increasing the attraction between the two solvents, the coil-to-globule transition shifts leftwards to smaller ε_{pA} and the magnitude of the shift increases.

We also perform numerical calculations on the reduced chain mean-square radius of gyration $\langle R_g^2\rangle_r$ as a function of χ_{pA} at x=0.2 using the Flory-type mean-field theory and present the results in Figs. 2(b) and 2(d) at χ_{pB}=−2 and 0.8 respectively. Likewise, we also include $\langle R_g^2\rangle_r$ as a function of χ_{pA} for a homopolymer chain in a single solvent A as the olive curve. We find that the theoretical predictions of $\langle R_g^2\rangle_r$ agree qualitatively with those obtained from the MC simulations. However, there are several main differences. First, for the single-solvent case with x=0, the $\langle R_g^2\rangle_r$ from the Flory-type mean-field theory increases monotonically while that in the MC simulation levels off with increasing the quality of solvent A. This difference is due to that the assumption of the Gaussian elastic energy in Eq. (8) ignores the finite extensibility of

https://doi.org/10.1007/s10118-025-3375-x

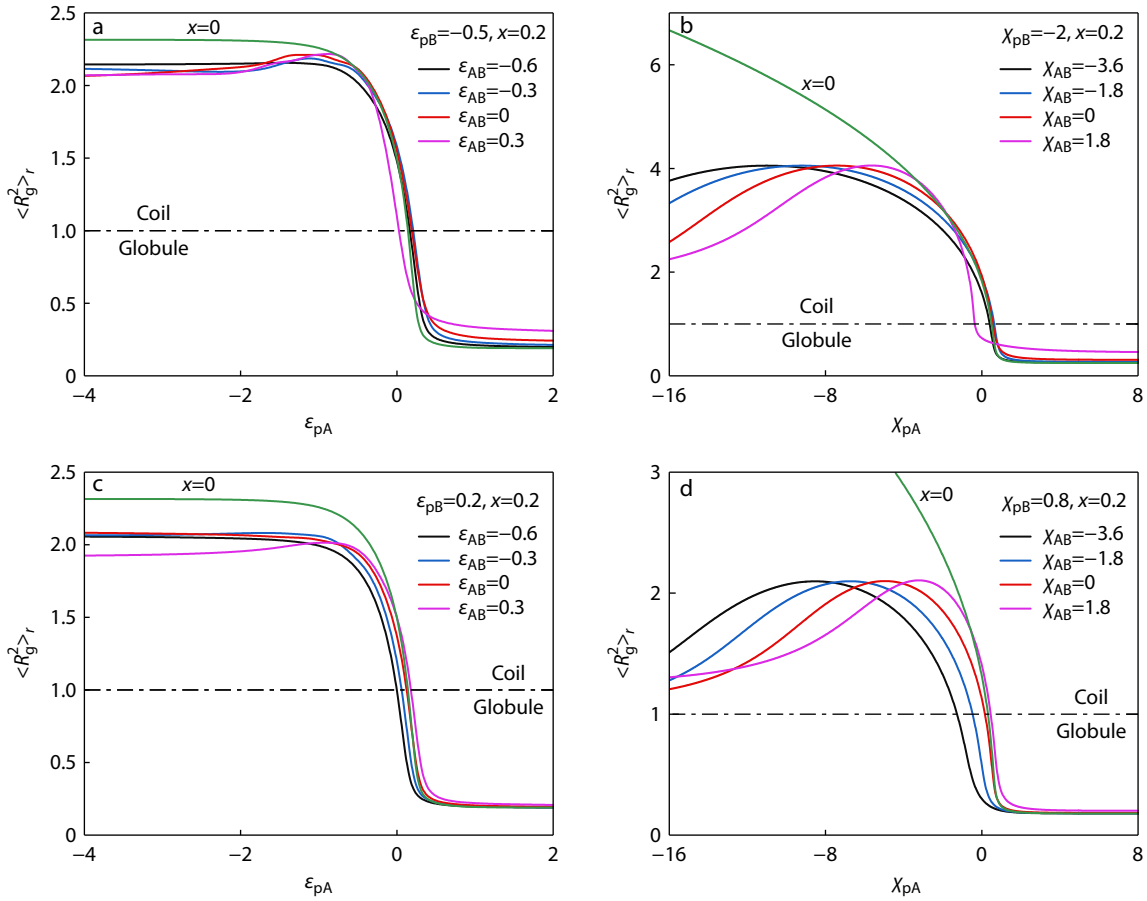

Fig. 2 The reduced chain mean-square radius of gyration $<R_g^2>_r$ as a function of ε_{pA} at various ε_{AB} and fixed ε_{pB}. Parts (a) and (c) are the MC simulation results at ε_{pB} =−0.5 and 0.2 respectively. Parts (b) and (d) are the numerical results using the Flory-type mean-field theory at χ_{pB} =−2 and 0.8, respectively. x=0.2, N=100, and V=40^3. The olive curves show $<R_g^2>_r$ as a function of ε_{pA} for a homopolymer chain in a single solvent A.

the chain. Because of the same reason, the chain size in the region of the coil state from the Flory-type mean-field theory is much higher than that from the MC simulations. Second, the decrease of $<R_g^2>_r$ at sufficiently negative χ_{pA} is much stronger than that from the MC simulation at negative ε_{pA}; this is probably due to the fact that the uniform distribution approximation of the concentrations of various species in the pervaded volume of the chain overestimates the enthalpic interactions. Nevertheless, the Flory-type mean-field theory qualitatively captures the essential ingredients, such as the chain conformation entropy, the mixing entropy of the two solvents, and the interactions among the three species, in governing the chain conformation of a homopolymer in mixed solvents.

With these results, we conclude that adding a small amount of solvent B, no matter whether it is good or poor, into a dilute homopolymer solution in solvent A, does not significantly affect the chain conformation if the solvent A is poor. However, when the solvent A is good to polymers, the addition of a small amount of solvent B can lead to a weak chain shrinkage and the degree of this shrinkage may increase with increasing the repulsion between the two solvents.

Effect of the Quality of Solvent A at Moderate *x*

Next let us examine how the dependences of the reduced chain mean-square radius of gyration $<R_g^2>$ on the quality of solvent A change at moderate compositions of the newly added solvent B. Taking x=0.5 as an example, in Fig. 3(a) we first present $<R_g^2>_r$ as a function of ε_{pA} at ε_{pB}=−0.5 from the MC simulations. Different from the curves in Fig. 2(a) with x=0.2, we find rather distinct non-monotonic dependence of $<R_g^2>_r$ on ε_{pA} in the mixed solvents at all studied values of ε_{AB}. Taking the case with ε_{AB}=0 as one example, the red curve in Fig. 3(a) shows that a homopolymer chain is in the globule state either when ε_{pA}>0.55 or when ε_{pA}<−2.75, but in the expanded coil state when −2.75<ε_{pA}<0.55. The largest value of $<R_g^2>_r$ is about 2.14 and is located at ε_{pA}≈−0.74. The chain collapse at positive ε_{pA} is due to the poor quality of solvent A. Under this condition, although there is an equal amount of good solvent B and poor solvent A in the solution, these two solvents tend to mix uniformly due to the mixing entropy and the chain must collapse to avoid the contact with solvent A. On the other hand, the collapse when ε_{pA}<−2.75 is due to the preferential attraction of polymers to solvent A over to solvent B. This chain collapse in mixtures of two good solvents is the celebrated co-nonsolvency effect in the literature.[15,20,26] These results are in good agreement with those by Zhang *et al.*[72] If we introduce an attraction between the two solvents, the blue and black solid curves in Fig. 2(a) (with ε_{AB}=−0.3 and −0.6) show that the globule region at positive ε_{pA} remains unchanged while the globule region at nega-

https://doi.org/10.1007/s10118-025-3375-x

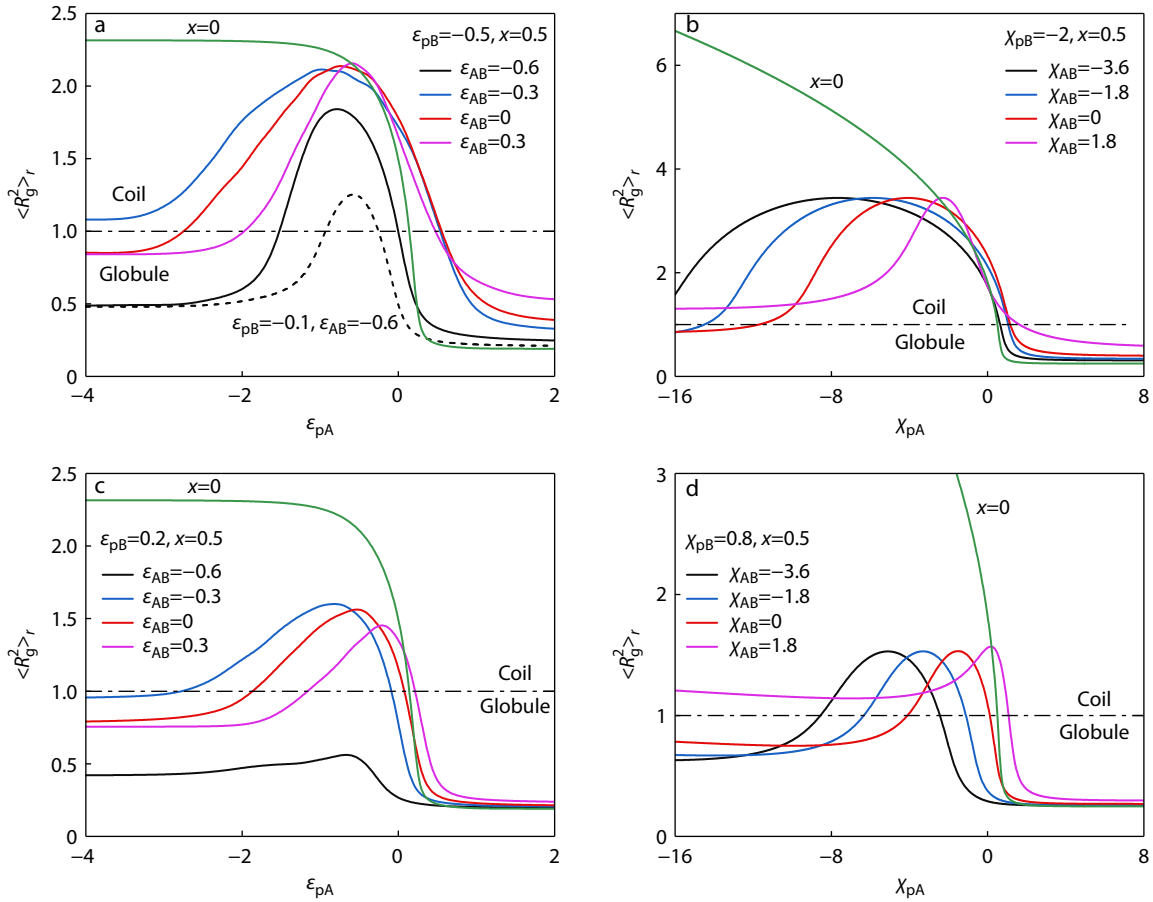

Fig. 3 The reduced chain mean-square radius of gyration $<R_g^2>_r$ as a function of ε_{pA} at various ε_{AB} and fixed ε_{pB}. Parts (a) and (c) are the MC simulation results at ε_{pB} =−0.5 and 0.2 respectively. Parts (b) and (d) are the numerical results using the Flory-type mean-field theory at χ_{pB} =−2 and 0.8, respectively. x=0.5, N=100, and V=40^3. The olive curves show $<R_g^2>_r$ as a function of ε_{pA} for a homopolymer chain in a single solvent A.

tive ε_{pA} first expands and then shrinks significantly. These reflect the synergist effects of ε_{AB} and ε_{pA} on the chain conformation. Moreover, we also present a case with ε_{AB}=0.3 to illustrate the effect of the repulsion between the two solvents; specifically, we find that the region of the coil state decreases significantly. Physically, this suggests that the introduction of a repulsion between the two solvents may lead to an expansion of the collapsed region. Moreover, the black dashed curve in Fig. 3(a) shows $<R_g^2>_r$ at ε_{pB} = −0.1 and ε_{AB} = −0.6. Comparing with the results at ε_{pB} = −0.5 and ε_{AB} = −0.6, we find that the region of the globule state increases significantly with increasing the quality of solvent B.

On the other hand, in Fig. 3(c) we show $<R_g^2>_r$ as a function of ε_{pA} at ε_{pB}=0.2 from the MC simulations. Different from that in Fig. 3(a), here solvent B is poor to polymer segments and a polymer chain is thus collapsed in pure solvent B. Again, with increasing the quality of solvent A (*i.e.*, decreasing ε_{pA}), $<R_g^2>_r$ first increases and then decrease gradually to a plateau value. For example, when ε_{AB}=0, the polymer chain is in the coil state when $-1.87< \varepsilon_{pA} <0.08$ and in the globule state when $\varepsilon_{pA}< -1.87$ or $\varepsilon_{pA}>0.08$. Again, the chain collapse when $\varepsilon_{pA}>0.08$ is due to the poor quality of both solvents A and B. The chain expansion when $-1.87< \varepsilon_{pA} <0.08$ is due to the good solvent A here; while solvent A is good and solvent B is poor to the polymer, the equal-molar mixture is a good solvent to polymer but the chain size is much smaller than those in pure solvent A. Finally, when $\varepsilon_{pA} < -1.87$, the quality of solvent A becomes very good. However, the chain collapses drastically in mixtures of this good solvent A and a poor solvent B. This non-trivial phenomenon is again due to that, in addition to the poor quality of solvent B, the molecules of good solvent A glue different monomers together and provide a further driving force for the chain collapse. This chain collapse shares the same physics as that in the co-nonsolvency effect discussed above. With the introduction of an attraction between solvents A and B, the blue curve with ε_{AB}=−0.3 suggests that the ε_{pA} region of the coil state shifts leftwards and the degree of shrinkage of the chain at sufficiently negative ε_{pA} decreases gradually. With further decreasing ε_{AB} to −0.6, the ε_{pA} region of the coil state vanishes completely and the chain is in the globule state over the entire range of ε_{pA}; in other words, if there is a strong attraction between the two solvents, a homopolymer chain tends to be collapsed no matter whether solvent A is good or not. On the other hand, when the interaction between solvents A and B is repulsive, the magenta curve in Fig. 3(a) shows that the region of the coil state shifts rightwards to larger ε_{pA}.

As a comparison, in Figs. 3(b) and 3(d) we present $<R_g^2>_r$ as a function of χ_{pA} at χ_{pB} = −2 and 0.8 respectively, using the Flory-type mean-field theory. The overall non-monotonic vari-

https://doi.org/10.1007/s10118-025-3375-x

ation features of $<R_g^2>_r$ along with χ_{pA} are qualitatively consistent with those for $<R_g^2>_r$ in MC simulations, with the following two differences. First, with increasing the attraction strength between the two solvents, the region of the coil state from the Flory-type mean field theory increases monotonically; on the contrary, the corresponding region of the coil state in the MC simulations first increases and then decreases. This is probably due to that the mean-field theory cannot capture the structure of strongly associative solvent mixtures. Second, when the two solvents are strongly repulsive (but still miscible), a chain may still collapse when ε_{pB} is sufficiently good in the MC simulations, but the Flory-type mean-field theory predicts that the chain adopts an expanded coil conformation therein.

Effect of the Quality of Solvent A at Large *x*

In this section, we will examine the conformational change of a homopolymer chain as a function of quality of solvent A when the composition of solvent B is large. By taking x=0.95 as an example, in Figs. 4(a) and 4(c) we show the reduced chain mean-square radius of gyration $<R_g^2>_r$ as a function of ε_{pA} at $\varepsilon_{pB} = -0.5$ and 0.2, respectively, obtained from MC simulations. When the solvent B is good to polymer (*i.e.*, $\varepsilon_{pB} = -0.5$), Fig. 4(a) shows that the chain is mainly swollen when ε_{pA} is positive or moderately negative but collapses rapidly to the globule state when ε_{pA} is sufficiently negative. For example, when $\varepsilon_{AB} = -0.6$, with increasing the quality of solvent A (*i.e.*, decreasing ε_{pA}), the chain first swells slightly and then decreases rapidly at $\varepsilon_{pA}<-1.8$ and enters the globule region when $\varepsilon_{pA}<-2.2$. The chain expansion at $\varepsilon_{pA}>-1.8$ is mainly due to the fact that the majority solvent B is good to the polymer. However, when $\varepsilon_{pA}<-2.2$ the collapse of the chain is mainly because that the minority solvent A (with its composition is only 5% here) is so good such that each molecule of solvent A plays a glue molecule that attracts several monomers together. Although this chain collapse will result in a chain conformation entropy penalty, the enthalpy gain is sufficiently large to lowest the total free energy. This issue is consistent with the result by Zhang and coworkers.[72] Moreover, we find that increasing ε_{AB} will shift the transition point of ε_{pA} to larger values, indicating that increasing the repulsion between two solvents can lead to the chain collapse. For example, at $\varepsilon_{pA}=-1.8$, the chain is in the coil state when $\varepsilon_{AB}=-0.3$, but it will collapse into the globule state when ε_{AB} increases to 0.3.

On the other hand, when the solvent B is poor to polymer (*e.g.*, ε_{pB}=0.2), Fig. 4(c) shows that the chain is always in the globule state over the entire range of ε_{pA}. This is mainly because poor solvent B here is the majority solvent. However, with decreasing ε_{pA}, the value of $<R_g^2>_r$ first increases and then decreases after a peak; this non-monotonic behaviour reflects the solvent quality effect of the minority solvent A on

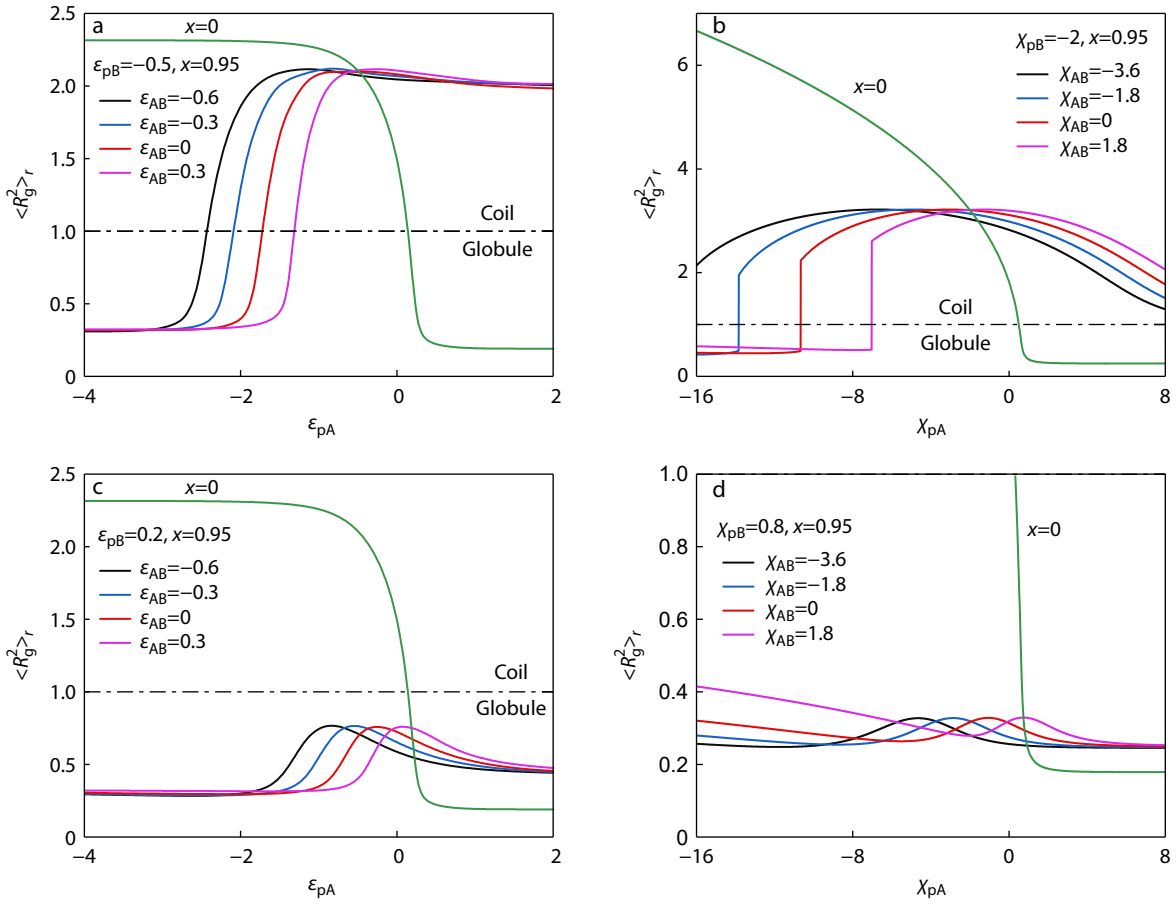

Fig. 4 The reduced chain mean-square radius of gyration $<R_g^2>_r$ as a function of ε_{pA} at various ε_{AB} and fixed ε_{pB}. Parts (a) and (c) are the MC simulation results at $\varepsilon_{pB}=-0.5$ and 0.2 respectively. Parts (b) and (d) are the numerical results using the Flory-type mean-field theory at $\chi_{pB}=-2$ and 0.8, respectively. x=0.95, N=100, and $V=40^3$. The olive curves show $<R_g^2>_r$ as a function of ε_{pA} for a homopolymer chain in a single solvent A.

https://doi.org/10.1007/s10118-025-3375-x

the chain conformation. Similar to the good solvent B case in Fig. 4(a), the location of the maximal $<R_g^2>_r$ shifts to larger values of ε_{pA} with increasing ε_{AB}.

With regard to the same system, we further calculate the reduced mean-square chain radius of gyration $<R_g^2>_r$ using the Flory-type mean-field theory. In Figs. 4(b) and 4(d), we present $<R_g^2>_r$ as a function of χ_{pA} at χ_{pB}=−2 and 0.8 respectively. The non-monotonic dependences of $<R_g^2>_r$ on χ_{pA} in Fig. 4(b) are qualitatively the same as those from MC simulations, but the chain collapse at large negative χ_{pA} is discontinuous, suggesting that the transition would be of first-order. However, by recalling that a thermodynamic phase transition can only take place in the thermodynamic limit, we regard this first-order collapse transition to be an artifact due to the mean-field approximation of the Flory-type mean-field theory. This artifact was also observed by de Gennes[84] in the coil-to-globule transition for a homopolymer chain in a single poor solvent. On the other hand, Fig. 4(d) shows that the non-monotonic behaviours of $<R_g^2>_r$ for the cases of poor solvent B also persists in the Flory-type mean-field theory, but the chain may expand slightly when χ_{pA} is sufficiently negative; again, this is due to the overestimation of the attraction between the solvent A and polymer segments therein.

CONCLUSIONS

In summary, based on a minimal lattice model, we have employed MC simulation and Flory-type mean-field theory to systematically study how the introduction of a second solvent B into a dilute homopolymer solution in solvent A affects the chain conformation. At fixed N=100 and V=40^3, the thermodynamics and structural properties of our systems are determined by the three interaction parameters between the three species, *i.e.*, ε_{pA}, ε_{pB}, ε_{AB}, and the composition of solvent B defined as $x = n_B/(n_A + n_B)$, where n_A and n_B are, respectively, the number of solvents A and B in the system. Specifically, we focus on the how the ε_{pA} dependence of the mean-square chain radius of gyration normalized by that in the single θ solvent $<R_g^2>_r$ varies in the presence of a second solvent B. Our main MC results are as follows:

(1) When the composition of solvent B is small, such as x=0.2, solvent A is the dominant solvent and the variation features of $<R_g^2>_r$ along with ε_{pA} remain roughly similar to those in pure solvent A, *i.e.*, the chain adopts the collapsed globule state at large ε_{pA} but the expanded coil state when ε_{pA} is small or negative. However, $<R_g^2>_r$ exhibits a slight shrinkage when the quality of solvent A is very good and the degree of shrinkage becomes more pronounced with decreasing the quality of solvent B or increasing the repulsion between solvents A and B. Moreover, for the case of poor solvent B, the location of the coil-to-globule transition in mixed solvents shifts to smaller ε_{pA} when ε_{AB} is negative but to larger ε_{pA} for positive ε_{AB}.

(2) When the composition of solvent B is moderate, such as x=0.5, $<R_g^2>_r$ exhibits a non-monotonic dependence on the quality of solvent A, no matter whether solvent B is good or poor. Specifically, the chain is in the collapsed state when solvent A is either sufficiently good or relatively poor to the polymer; at intermediate range of ε_{pA}, the chain adopts the expanded coil conformation. The chain collapse in the equal-molar mixture of good solvent B and poor solvent A is due to the interplay between the mixing entropy that prefers the uniform distribution of the two solvents and the tendency to minimize the unfavourable contact between polymer segments and solvents A. On the other hand, in mixtures of a good solvent B and a solvent A much better than B, the chain collapses because of that the solvent B plays the glue species that bind several monomers together; this is the co-nonsolvency effect that results from the preferential attraction of polymers to one of the two solvents. Moreover, with increasing the attraction between the two solvents, the region of the coil state first expands and then shrinks. On the other hand, with increasing the repulsion between the two solvents, the region of the coil state shrinks gradually.

(3) When the composition of solvent B is high, such as x=0.95, solvent B is the majority while solvent A is the minority. For the case of good solvent B, the chain collapses when the quality of solvent A becomes very good but adopts an expanded coil state for other qualities of solvent A. Again, the chain collapse at sufficiently good solvent A is due to that one solvent molecule of type A connects several monomers together. The value of ε_{pA} where the chain collapses decreases with decreasing ε_{AB}. On the other hand, for the case of poor solvent B, the chain remains in the collapsed globule state over the entire range of the quality of solvent A. However, $<R_g^2>_r$ also exhibits a non-monotonic dependence on ε_{pA}, and the location of the maximal $<R_g^2>_r$ shifts to larger value of ε_{pA} with increasing ε_{AB}.

For the above three cases, we have also performed numerical calculations using the Flory-type mean-field theory. We observe qualitatively the same features in the variation of $<R_g^2>_r$ along with the quality of solvent A for most cases; this suggests that this mean-field theory indeed captures the main physics on the conformation of a homopolymer chain in mixtures of binary solvents. However, there are several qualitative differences, such as the variation in the region of the coil state with χ_{pA} at negative χ_{AB}, and several other quantitative differences. These differences result from the inaccurate treatment of the conformation entropy as well as the mean-field treatment of the interactions among the three species. For example, the deformation free energy due to chain conformation does not consider the finite extensibility effect, and thus, lead to a continuous increase of the chain size with increasing the solvent quality, in contrast to the saturation of the chain size therein. Nevertheless, the Flory-type mean-field theory still serves as a reasonable method to elucidate the conformation transition of a homopolymer chain in mixtures of binary solvents, due to its high computational efficiency.

Currently, in experiments the radius of gyration of a single PNIPAM chain in mixtures of water and methanol was usually measured at fixed room temperature.[20] In view of that the solvent quality of water decreases with increasing temperature while that of methanol depends weakly on temperature, one may assume that water is solvent A and methanol is solvent B in our system. This suggests that, it is possible to verify our predictions by measuring the radius of gyration of a single PNIPAM chain at different temperatures, with the composition of methanol fixed at various values, by using techniques such as the neutron/laser scattering or fluorescence labeling. We hope our simulation results presented here will

https://doi.org/10.1007/s10118-025-3375-x

motivate further experimental work in this direction.

Finally, the MC methods used in this work can be directly generalized to examine the chain conformation and phase behaviours of homopolymer solutions at finite concentrations. Moreover, it is expected that other types of polymers, such as polymer brushes, polymer thin films, and block copolymers also may exhibit very rich phenomenon in mixtures of binary solvents. A systematic investigation on the chain conformation and phase behaviours of these systems will greatly broaden the horizon for the rational design of various functional polymeric materials. Our work here represents a demonstration in this aspect, and we hope more efforts will be made along this direction in the future.

Conflict of Interests

The authors declare no interest conflict.

Data Availability Statement

The data supporting the findings of this study are available from the corresponding author upon reasonable request.

ACKNOWLEDGMENTS

This work was financially supported by the National Natural Science Foundation of China (Nos. 22473024, 22073016 and 21803011) and the award of Shanghai Dongfang Scholar.

REFERENCES

1 Gao, S.; Tang, G.; Hua, D.; Xiong, R.; Han, J.; Jiang, S.; Zhang, Q.; Huang, C. Stimuli-responsive bio-based polymeric systems and their applications. *J. Mater. Chem. B* **2019**, *7*, 709–729.
2 Stuart, M. A. C.; Huck, W. T.; Genzer, J.; Müller, M.; Ober, C.; Stamm, M.; Sukhorukov, G. B.; Szleifer, I.; Tsukruk, V. V.; Urban, M. Emerging applications of stimuli-responsive polymer materials. *Nat. Mater.* **2010**, *9*, 101–113.
3 Morimoto, N.; Qiu, X.-P.; Winnik, F. M.; Akiyoshi, K. Dual stimuli-responsive nanogels by self-assembly of polysaccharides lightly grafted with thiol-terminated poly(*N*-isopropylacrylamide) chains. *Macromolecules* **2008**, *41*, 5985–5987.
4 Zhao, X.-q.; Wang, T.-x.; Liu, W.; Wang, C.-d.; Wang, D.; Shang, T.; Shen, L.-h.; Ren, L. Multifunctional Au@ IPN-pNIPAAm nanogels for cancer cell imaging and combined chemo-photothermal treatment. *J. Mater. Chem.* **2011**, *21*, 7240–7247.
5 Wen, T.; Gao, Y.; Zhou, J.; Qiu, J.; Wang, S.; Loos, J.; Wang, D.; Dong, X. Fast fabrication of porous amphiphilic polyamides *via* nonconventional evaporation induced phase separation. *ACS Macro Lett.* **2023**, *12*, 697–702.
6 Radjabian, M.; Abetz, V. Advanced porous polymer membranes from self-assembling block copolymers. *Prog. Polym. Sci.* **2020**, *102*, 101219.
7 Wang, D. M.; Lai, J. Y. Recent advances in preparation and morphology control of polymeric membranes formed by nonsolvent induced phase separation. *Curr. Opin. Chem. Eng.* **2013**, *2*, 229–237.
8 Vogel, M. J.; Steen, P. H. Capillarity-based switchable adhesion. *Proc. Natl. Acad. Sci.* **2010**, *107*, 3377–3381.
9 Lee, H.; Lee, B. P.; Messersmith, P. B. A reversible wet/dry adhesive inspired by mussels and geckos. *Nature* **2007**, *448*, 338–341.
10 Rose, S.; Prevoteau, A.; Elzière, P.; Hourdet, D.; Marcellan, A.; Leibler, L. Nanoparticle solutions as adhesives for gels and biological tissues. *Nature* **2014**, *505*, 382–385.
11 Wu, C.; Wang, X. Globule-to-coil transition of a single homopolymer chain in solution. *Phys. Rev. Lett.* **1998**, *80*, 4092–4094.
12 De Gennes, P. Kinetics of collapse for a flexible coil. *J. Physique Lett.* **1985**, *46*, 639–642.
13 Halperin, A.; Goldbart, P. M. Early stages of homopolymer collapse. *Phys. Rev. E* **2000**, *61*, 565–573.
14 Lifshitz, I.; Grosberg, A. Y.; Khokhlov, A. Some problems of the statistical physics of polymer chains with volume interaction. *Rev. Mod. Phys.* **1978**, *50*, 683–713.
15 Wang, Z. G. 50th Anniversary perspective: polymer conformation: a pedagogical review. *Macromolecules* **2017,** *50*, 9073–9114.
16 Grosberg, A. Y.; Kuznetsov, D. Quantitative theory of the globule-to-coil transition. 1. Link density distribution in a globule and its radius of gyration. *Macromolecules* **1992**, *25*, 1970–1979.
17 Shultz, A.; Flory, P. Polymer chain dimensions in mixed-solvent media. *J. Polym Sci.* **1955**, *15*, 231–242.
18 Brochard, F.; De Gennes, P. Collapse of one polymer coil in a mixture of solvents. *Ferroelectrics* **1980**, *30*, 33–47.
19 Schild, H. G.; Muthukumar, M.; Tirrell, D. A. Cononsolvency in mixed aqueous solutions of poly(*N*-isopropylacrylamide). *Macromolecules* **1991**, *24*, 948–952.
20 Zhang, G.; Wu, C. The water/methanol complexation induced reentrant coil-to-globule-to-coil transition of individual homopolymer chains in extremely dilute solution. *J. Am. Chem. Soc.* **2001**, *123*, 1376–1380.
21 He, L.; Cheng, G.; Melnichenko, Y. B. Partial collapse and reswelling of a polymer in the critical demixing region of good solvents. *Phys. Rev. Lett.* **2012**, *109*, 067801.
22 Zhang, Q.; Hoogenboom, R. Polymers with upper critical solution temperature behavior in alcohol/water solvent mixtures. *Prog. Polym. Sci.* **2015**, *48*, 122–142.
23 Budkov, Y. A.; Kolesnikov, A. Statistical description of co-nonsolvency suppression at high pressures. *Soft Matter* **2017**, *13*, 8362–8367.
24 Mukherji, D.; Marques, C. M.; Stuehn, T.; Kremer, K. Depleted depletion drives polymer swelling in poor solvent mixtures. *Nat. Commun.* **2017**, *8*, 1374.
25 Zheng, X.; Anisimov, M. A.; Sengers, J. V.; He, M. Unusual transformation of polymer coils in a mixed solvent close to the critical point. *Phys. Rev. Lett.* **2018**, *121*, 207802.
26 Mukherji, D.; Marques, C. M.; Kremer, K. Polymer collapse in miscible good solvents is a generic phenomenon driven by preferential adsorption. *Nat. Commun.* **2014**, *5*, 4882.
27 Hao, J.; Cheng, H.; Butler, P.; Zhang, L.; Han, C. C. Origin of cononsolvency, based on the structure of tetrahydrofuran-water mixture. *J. Chem. Phys.* **2010**, *132*, 154902.
28 Bharadwaj, S.; Niebuur, B. J.; Nothdurft, K.; Richtering, W.; van der Vegt, N. F.; Papadakis, C. M. Cononsolvency of thermoresponsive polymers: where we are now and where we are going. *Soft Matter* **2022**, *18*, 2884–2909.
29 Wang, F.; Shi, Y.; Luo, S.; Chen, Y.; Zhao, J. Conformational transition of poly(*N*-isopropylacrylamide) single chains in its cononsolvency process: a study by fluorescence correlation spectroscopy and scaling analysis. *Macromolecules* **2012**, *45*, 9196–9204.
30 Zuo, T.; Ma, C.; Jiao, G.; Han, Z.; Xiao, S.; Liang, H.; Hong, L.; Bowron, D.; Soper, A.; Han, C. C. Water/cosolvent attraction induced phase separation: a molecular picture of cononsolvency. *Macromolecules* **2019**, *52*, 457–464.
31 Jia, D.; Muthukumar, M.; Cheng, H.; Han, C. C.; Hammouda, B.

Concentration fluctuations near lower critical solution temperature in ternary aqueous solutions. *Macromolecules* **2017**, *50*, 7291–7298.
32 Jia, D.; Zuo, T. S.; Rogers, S.; Cheng, H.; Hammouda, B.; Han, C. C. Re-entrance of poly(*N*,*N*-diethylacrylamide) in D_2O/*d*-ethanol mixture at 27 °C. *Macromolecules* **2016**, *49*, 5152–5159.
33 Hore, M. J.; Hammouda, B.; Li, Y.; Cheng, H. Hore, M. J. A.; Hammouda, B.; Li, Y. Y.; Cheng, H. Co-nonsolvency of poly(*n*-isopropylacrylamide) in deuterated water/ethanol mixtures. *Macromolecules* **2013**, *46*, 7894–7901.
34 Kreuzer, L. P.; Lindenmeir, C.; Geiger, C.; Widmann, T.; Hildebrand, V.; Laschewsky, A.; Papadakis, C. M.; Muller-Buschbaum, P. Poly(sulfobetaine) versus poly(*N*-isopropylmethacrylamide): co-nonsolvency-type behavior of thin films in a water/methanol atmosphere. *Macromolecules* **2021**, *54*, 1548–1556.
35 Winnik, F. M.; Ringsdorf, H.; Venzmer, J. Methanol-water as a co-nonsolvent system for poly(*N*-isopropylacrylamide). *Macromolecules* **1990**, *23*, 2415–2416.
36 Winnik, F. M.; Ottaviani, M. F.; Bossmann, S. H.; Garcia-Garibay, M.; Turro, N. J. Consolvency of poly(*N*-isopropylacrylamide) in mixed water-methanol solutions: a look at spin-labeled polymers. *Macromolecules* **1992**, *25*, 6007–6017.
37 Sun, S.; Wu, P. Role of water/methanol clustering dynamics on thermosensitivity of poly(*N*-isopropylacrylamide) from spectral and calorimetric insights. *Macromolecules* **2010**, *43*, 9501–9510.
38 Hofmann, C. H.; Plamper, F. A.; Scherzinger, C.; Hietala, S.; Richtering, W. Cononsolvency revisited: solvent entrapment by *N*-isopropylacrylamide and *N, N*-diethylacrylamide microgels in different water/methanol mixtures. *Macromolecules* **2013**, *46*, 523–532.
39 Fukai, T.; Shinyashiki, N.; Yagihara, S.; Kita, R.; Tanaka, F. Phase behavior of co-nonsolvent systems: poly(*N*-isopropylacrylamide) in mixed solvents of water and methanol. *Langmuir* **2018**, *34*, 3003–3009.
40 Mills, C. E.; Ding, E.; Olsen, B. D. Cononsolvency of elastin-like polypeptides in water/alcohol solutions. *Biomacromolecules* **2019**, *20*, 2167–2173.
41 Kyriakos, K.; Philipp, M.; Adelsberger, J.; Jaksch, S.; Berezkin, A. V.; Lugo, D. M.; Richtering, W.; Grillo, I.; Miasnikova, A.; Laschewsky, A. Cononsolvency of water/methanol mixtures for PNIPAM and PS-*b*-PNIPAM: pathway of aggregate formation investigated using time-resolved SANS. *Macromolecules* **2014**, *47*, 6867–6879.
42 Ko, C. H.; Henschel, C.; Meledam, G. P.; Schroer, M. A.; Guo, R.; Gaetani, L.; Müller-Buschbaum, P.; Laschewsky, A.; Papadakis, C. M. Co-nonsolvency effect in solutions of poly(methyl methacrylate)-*b*-poly(*N*-isopropylacrylamide) diblock copolymers in water/methanol mixtures. *Macromolecules* **2021**, *54*, 5825–5837.
43 Zhang, Y. Y.; Jia, X. M.; Shi, R.; Li, S. J.; Zhao, H.; Qian, H. J.; Lu, Z. Y. Synthesis of polymer single-chain nanoparticle with high compactness in cosolvent condition: a computer simulation study. *Macromol. Rapid Commun.* **2020**, *41*, 1900665.
44 Sommer, J. U. Adsorption–attraction model for co-nonsolvency in polymer brushes. *Macromolecules* **2017**, *50*, 2219–2228.
45 Galuschko, A.; Sommer, J. U. Co-nonsolvency response of a polymer brush: a molecular dynamics study. *Macromolecules* **2019**, *52*, 4120–4130.
46 Smook, L. A.; Eck, G. C. R. V.; Beer, S. D. Friends, foes, and favorites: relative interactions determine how polymer brushes absorb vapors of binary solvents. *Macromolecules* **2020**, *53*, 10898–10906.
47 Yong, H.; Rauch, S.; Eichhorn, K. J.; Uhlmann, P.; Fery, A.; Sommer, J. U. Cononsolvency transition of polymer brushes: a combined experimental and theoretical study. *Materials* **2018**, *11*, 991.
48 Park, G.; Jung, Y. Many-chain effects on the co-nonsolvency of polymer brushes in a good solvent mixture. *Soft Matter* **2019**, *15*, 7968–7980.
49 Yong, H.; Bittrich, E.; Uhlmann, P.; Fery, A.; Sommer, J. U. Co-nonsolvency transition of poly(*N*-isopropylacrylamide) brushes in a series of binary mixtures. *Macromolecules* **2019**, *52*, 6285–6293.
50 Yong, H.; Merlitz, H.; Fery, A.; Sommer, J. U. Polymer brushes and gels in competing solvents: the role of different interactions and quantitative predictions for poly(*N*-isopropylacrylamide) in alcohol–water mixtures. *Macromolecules* **2020**, *53*, 2323–2335.
51 Amiya, T.; Hirokawa, Y.; Hirose, Y.; Li, Y.; Tanaka, T. Reentrant phase transition of *N*-isopropylacrylamide gels in mixed solvents. *J. Chem. Phys.* **1987**, *86*, 2375–2379.
52 Wang, Z.; Yin, Y.; Jiang, R.; Li, B. Morphological transformations of diblock copolymers in binary solvents: a simulation study. *Front. Phys.* **2017**, *12*, 128201.
53 Fernández-Piérola, I.; Horta, A. Co-nonsolvency of PMMA. *Polym. Bull.* **1980**, *3*, 273–278.
54 Winnik, F. M.; Ottaviani, M. F.; Bossmann, S. H.; Pan, W.; Garcia-Garibay, M.; Turro, N. J. Cononsolvency of poly(*N*-isopropylacrylamide): a look at spin-labeled polymers in mixtures of water and tetrahydrofuran. *Macromolecules* **1993**, *26*, 4577–4585.
55 Tanaka, F.; Koga, T.; Winnik, F. M. Temperature-responsive polymers in mixed solvents: competitive hydrogen bonds cause cononsolvency. *Phys. Rev. Lett.* **2008**, *101*, 028302.
56 Osaka, N.; Shibayama, M. Pressure effects on cononsolvency behavior of poly(*N*-isopropylacrylamide) in water/DMSO mixed solvents. *Macromolecules* **2012**, *45*, 2171–2174.
57 Rodríguez-Ropero, F.; Hajari, T.; van der Vegt, N. F. Mechanism of polymer collapse in miscible good solvents. *J. Phys. Chem. B* **2015**, *119*, 15780–15788.
58 Pica, A.; Graziano, G. An alternative explanation of the cononsolvency of poly(*N*-isopropylacrylamide) in water-methanol solutions. *Phys. Chem. Chem. Phys.* **2016**, *18*, 25601–25608.
59 Budkov, Y. A.; Kolesnikov, A.; Kalikin, N.; Kiselev, M. A statistical theory of coil-to-globule-to-coil transition of a polymer chain in a mixture of good solvents. *Europhys. Lett.* **2016**, *114*, 46004.
60 Dudowicz, J.; Freed, K. F.; Douglas, J. F. Relation between solvent quality and phase behavior of ternary mixtures of polymers and two solvents that exhibit cononsolvency. *J. Phys. Chem. B* **2016**, *120*, 5753–5758.
61 Mochizuki, K.; Pattenaude, S. R.; Ben-Amotz, D. Influence of cononsolvency on the aggregation of tertiary butyl alcohol in methanol–water mixtures. *J. Am. Chem. Soc.* **2016**, *138*, 9045–9048.
62 Dalgicdir, C.; Rodríguez-Ropero, F.; van der Vegt, N. F. Computational calorimetry of PNIPAM cononsolvency in water/methanol mixtures. *J. Phys. Chem. B* **2017**, *121*, 7741–7748.
63 Mukherji, D.; Marques, C. M.; Kremer, K. Collapse in two good solvents, swelling in two poor solvents: defying the laws of polymer solubility. *J. Phys.: Condens. Matter* **2017**, *30*, 024002.
64 Pica, A.; Graziano, G. On the cononsolvency behaviour of hydrophobic clusters in water-methanol solutions. *Phys. Chem. Chem. Phys.* **2018**, *20*, 7230–7235.
65 Zhang, J.; Mukherji, D.; Kremer, K.; Daoulas, K. C. Studying polymer solutions with particle-based models linked to classical density functionals: co-non-solvency. *Soft Matter* **2018**, *14*, 9282–9295.
66 Bharadwaj, S.; van der Vegt, N. F. Does preferential adsorption drive cononsolvency. *Macromolecules* **2019**, *52*, 4131–4138.
67 Zhang, X.; Zong, J.; Meng, D. A unified understanding of the cononsolvency of polymers in binary solvent mixtures. *Soft Matter* **2020**, *16*, 7789–7796.
68 Bharadwaj, S.; Nayar, D.; Dalgicdir, C.; van der Vegt, N. F. A

cosolvent surfactant mechanism affects polymer collapse in miscible good solvents. *Commun. Chem.* **2020**, *3*, 165.
69 Mukherji, D.; Marques, C. M.; Stuehn, T.; Kremer, K. Co-non-solvency: mean-field polymer theory does not describe polymer collapse transition in a mixture of two competing good solvents. *J. Chem. Phys.* **2015**, *142*, 114903.
70 Dudowicz, J.; Freed, K. F.; Douglas, J. F. Communication: cosolvency and cononsolvency explained in terms of a Flory-Huggins type theory. *J. Chem. Phys.* **2015**, *143*, 131101.
71 Chen, X.; Feng, W.; Han, X.; Liu, H. Possible way to study cononsolvency in confinement: a lattice density functional theory approach. *Langmuir* **2017**, *33*, 11446−11456.
72 Zhang, P.; Wang, Z.; Wang, Z.-G. Conformation transition of a homopolymer chain in binary mixed solvents. *Macromolecules* **2022**, *56*, 153−165.
73 Zhang, P. Phase separation of homopolymers in binary mixed solvents— the co -nonsolvency effect. *Macromolecules* **2024**, *57*, 4298−4311.
74 Zhang, P. Phase separation of homopolymers in binary mixed solvents: the co-solvency effect. *Macromolecules* **2025**, *58*, 2472−2483.
75 Tanaka, F.; Koga, T.; Kojima, H.; Xue, N.; Winnik, F. M. Preferential adsorption and co-nonsolvency of thermoresponsive polymers in mixed solvents of water/methanol. *Macromolecules* **2011**, *44*, 2978−2989.
76 Magda, J.; Fredrickson, G.; Larson, R.; Helfand, E. Dimensions of a polymer chain in a mixed solvent. *Macromolecules* **1988**, *21*, 726−732.
77 Wang, F.; Landau, D. P. Efficient, multiple-range random walk algorithm to calculate the density of states. *Phys. Rev. Lett.* **2001**, *86*, 2050−2053.
78 Wang, F.; Landau, D. P. Determining the density of states for classical statistical models: a random walk algorithm to produce a flat histogram. *Phys. Rev. E* **2001**, *64*, 056101.
79 Budkov, Y. A.; Kiselev, M. Flory-type theories of polymer chains under different external stimuli. *J. Phys.: Condens. Matter* **2017**, *30*, 043001.
80 Budkov, Y. A.; Kolesnikov, A. Models of the conformational behavior of polymers in mixed solvents. *Polym. Sci. Ser. C* **2018**, *60*, 148−159.
81 Yang, D.; Wang, Q. Unified view on the mean-field order of coil-globule transition. *ACS Macro Lett.* **2013**, *2*, 952−954.
82 Rampf, F.; Paul, W.; Binder, K. On the first-order collapse transition of a three-dimensional, flexible homopolymer chain model. *Europhys. Lett.* **2005**, *70*, 628.
83 Taylor, M. P.; Paul, W.; Binder, K. Phase transitions of a single polymer chain: a Wang–Landau simulation study. *J. Chem. Phys.* **2009,** *131*, 114907.
84 de Gennes, P. G. Collapse of a polymer chain in poor solvents. *J. Physique Lett.* **1975**, *36*, 55−57.

https://doi.org/10.1007/s10118-025-3375-x